Author/s:
Maclean, FL;Ims, GM;Horne, MK;Williams, RJ;Nisbet, DR

Title:
A Programmed Anti-Inflammatory Nanoscaffold (PAIN) as a 3D Tool to Understand the Brain Injury Response

Date:
2018-12-13

Citation:
Maclean, F. L., Ims, G. M., Horne, M. K., Williams, R. J. & Nisbet, D. R. (2018). A Programmed Anti-Inflammatory Nanoscaffold (PAIN) as a 3D Tool to Understand the Brain Injury Response. Advanced Materials, 30 (50), https://doi.org/10.1002/adma.201805209.

Persistent Link:
https://hdl.handle.net/11343/284652

DOI: 10.1002/((please add manuscript number))

Article type: Communication

Programmed anti-inflammatory nanoscaffold (PAIN) as a 3D tool to understand the brain injury response.

Francesca L. Maclean, Georgina M. Ims, Malcolm K. Horne, Richard J. Williams and David R. Nisbet[*]

Dr R.J. Williams and Associate Professor D. R. Nisbet had equal contribution.

Dr F. L. Maclean[1], Ms G. M. Ims[1], Professor M. K. Horne[2,3], Dr R. J. Williams[4,5], and Associate Professor David R. Nisbet[1,2,5]

[1]Laboratory of Advanced Biomaterials, Research School of Engineering, The Australian National University, Canberra, Australia, 2601. [2]Florey Institute of Neuroscience and Mental Health, University of Melbourne, Parkville, Australia, 3052. [3]Department of Medicine, University of Melbourne, St Vincent's Hospital, Fitzroy, Australia, 3065. [4]School of Engineering, RMIT University, Melbourne, Australia, 3000. [5]BioFab3D, St Vincent's Hospital, Fitzroy, Australia, 3065.

Corresponding Author: E-mail: david.nisbet@anu.edu.au, Associate Professor D. R. Nisbet[1,2,5], richard.williams@rmit.edu.au, Dr R. J. Williams[4,5]

Keywords: 3D cell culture, nanoscaffolds, regenerative medicine, disease modeling, inflammation

Abstract:

Immunology is the next frontier of nano/biomaterial science research, with the immune system determining the degree of tissue repair. However, the complexity of the inflammatory response represents a significant challenge that is essential to understand for the development of future therapies. Cell-instructive 3D culture environments are critical to improve our understanding of the link between the behaviour and morphology of inflammatory cells and to remodel their response to injury. This study has taken two recent high-profile innovations – functional peptide-based hydrogels, and the inclusion of anti-inflammatory agents via co-assembly – to make a programmed anti-inflammatory nanoscaffold (PAIN) with unusual and valuable properties that allows tissue independent switching of the inflammatory cascade. Here, extraordinary durability of the anti-inflammatory agent allows, for the first time, the development of a 3D culture system that maintains the growth and cytoskeletal reorganisation of brain tissue, whilst also facilitating the trophic behaviour of brain cells for 22 days *in vitro*. Notably, this behavior was confirmed within an active scar site, due to the unprecedented resilience to the presence of inflammatory cells and enzymes in the brain. Efficacy of the culture system is demonstrated via novel insights about inflammatory cell behaviour, which would be impossible to obtain via *in vivo* experimentation.

Main text:

The merging of the fields of immunology, tissue engineering and regenerative medicine represents the next frontier of medical research, whereby programmable materials can be engineered to remodel and regulate immune function.[1] Recently, the engineering of such novel multicomponent and nanocellular scaffolds and 3D culture systems [2] has been recognised within a variety of applications, along with their inherent ability to study disease progression and the efficacy of therapeutic intervention.[3] Here, we have engineered a programmed anti-inflammatory nanoscaffold (PAIN) as an ideal tool to separate the immune, inflammatory and cellular response to understand the *in vivo* response to brain insult. We have demonstrated the ability of our nanoscaffold to reprogram the behaviour of existing endogenous immune cells within the brain, astrocytes, to promote the networked cobblestone morphology only observed in astrocytes in a healthy uninjured brain. In this study astrocytes are a unique and deliberate target, due to their critical secretome, structural support and maintenance of the blood-brain-barrier. [4]

Astrocytes are a multifunctional inflammatory cell type found throughout the brain.[5] Their physiological functions are essential within a healthy brain, but they are also core components in inflammation and in determining the brain's cellular response to injury.[6] Post insult, they play an important role in the stabilisation and regeneration of the brain parenchyma,[5] and as such are a valuable therapeutic target to facilitate improved recovery. Although the complex roles and activity of astrocytes remain poorly understood, [7] their therapeutic value highlights the need for *in vitro* investigation of these cells and their response to treatments, to develop better therapies for brain injury.

Astrocytes in the uninjured brain are highly networked cells linking blood vessels and neurones and present as a cobblestone morphology; yet currently available two-dimensional cell culture environments cannot allow them to reproduce this organisation, as they do not recapitulate the dynamic, three-dimensional extracellular environment found in brain tissue. Under two-dimensional culture astrocytes present as stellated, hypertrophied cells, the same morphology of as reactive astrocytes within the injured brain. In-order to replicate some of the features of the three-dimensional extracellular environment electrospun nanofiber scaffolds have been used, [8] including to study astrocyte morphology and behaviour *in vitro.* These scaffolds have been demonstrated to successfully maintaining cytotrophic or "pro-survival" phenotypes of astrocytes, decreasing cellular stress and promoting the expression of intermediate filament proteins typically used to characterise reactive astrocytes.[9-12] However, it is likely that these studies will not be readily translated into therapies because the geometrical constraints of nanofiber scaffold membranes[13] prevent the material construct from easily filling the post trauma cavity and thus forming intimate contact with the surrounding parenchyma. A nanofiber scaffold that could flow to fill odd-shaped cavities within lesions, while maintaining morphological and biological functionality, is required for *in vivo*

deployment. Indeed *in vitro* studies should be performed on scaffolds that can be deployed if they are to have clinical relevance of the outcomes.[14] For this reason the swollen and hydrated networks of certain hydrogels have gained recent attention because they address the requirement of being 3D cell culture systems, with naturally-derived and synthetic hydrogels (including collagen, agarose, Matrigel, and poly(ethylene glycol)) being explored.[15] However, many of these materials, particularly the naturally derived biomaterials, are not chemically well defined, and thus cannot be readily reproduced nor do they have nanofibrous morphology that truly mimics the extracellular matrix (ECM). As a consequence, composite materials using hydrogels and nanofibers [16] or nanospheres, [17] nanofibrous structures, [18] such as those formed by the self-assembly of peptides, [19, 20, 21] amino acid peptide-based hydrogels, [22] or decellularized brain tissue [23] have been proposed. For more information about the utilization of such materials the interested reader is referred to the following excellent reviews on self-assembling peptides [24] and amyloids. [25]

Here, we investigate a programmed Fmoc-self assembled peptide (Fmoc-SAP) hydrogel, designed to mimic the nanofibrous structure of the brain's ECM, while presenting high density epitopes such as RGD, IKVAV, and YISGR on the nanofibril surface.[21, 26] We have shown that Fmoc-SAPs can be engineered to present (both *in vitro* and *in vivo*) growth factors,[27] developmentally important proteoglycans,[28] polysaccharides,[20] and viral vectors[29] from a shear thinning hydrogel which can make intimate contact with tissue surrounding a void.[30] Of particular interest for neural applications is Fmoc-DIKVAV, a mimic of the sequence IKVAV, which is a key component of laminin (the major constituent of the brain's ECM) and subsequently referred to here as Fmoc-DLam. We then modified Fmoc-DLam to function as a tissue engineering construct that was capable of presenting an anti-inflammatory microenvironment through co-assembly with the anti-inflammatory and anti-proliferative sulphated polysaccharide, fucoidan (Fmoc-DLamFuc). Because this compound

downregulates pro-inflammatory cytokines by inhibiting NF-κB, Akt, and MAPK activation in LPS-stimulated microglial cells, as well as inducing apoptosis in epithelial cancer cells, fucoidan may also modulate the inflammatory behaviour of astrocytes.[20, 31] We have previously shown that fucoidan is incorporated strongly to the surface of the fibrils during the assembly process to a fibronectin mimicking sequence[20] and that galactose polymers downregulate the inflammatory behaviour of astrocytes.[9, 13, 32] Therefore, we hypothesise that fucoidan incorporated with our Fmoc-DLam molecular hydrogel would also modulate the inflammatory behaviour of astrocytes allowing us, for the first time, to study their responses to traumatic brain injury both *in vitro*, and *in vivo*. Indeed, this was the case, when we cultured astrocytes *in vitro* on the nanoscaffold they were enabled to form a cobblestone morphology, the same morphology to those within the uninjured brain. We believe, this type of cytoskeletal presentation, shifting from stellated, hypertrophied cells to "*in vivo* like" morphologies have never been reported *in vitro* previously. We now refer to this phenomenon as the 'network formation' of astrocytes. For further discussion about the significance of astrocyte network formation and the associated cytoskeletal reorganisation and its influence on neurones, please refer to supplementary information.

Here, we demonstrate dual functionalities of the programmed anti-inflammatory nanoscaffold (PAIN) system consisting of Fmoc-DLam and Fmoc-DLamFuc *in vitro.* We report that Fmoc-DLam functions as a long term (up 24 days) three-dimensional culture environment for astrocytes, as shown by comparison with morphologies observed *in vivo*, promoting the cells to form a biologically relevant network in 3D. We then program the system to mimic the inflammatory environment, challenging the astrocytes with LPS or IL-1α. Finally, the Fmoc-DLamFuc 3D model allows us to then probe the anti-proliferative effects of fucoidan on these stimulated cells. This provides a solid foundation for *in vitro* investigation of astrocytes using a 3D, biologically relevant biomaterial system

with a programmable inflammatory milieu, which will improve translation of *in vitro* results into *in vivo* settings. We demonstrate the efficacy of our system, gaining novel insights of astrocyte behaviour that would be impossible to obtain through *in vivo* experimentation. Furthermore, we have illustrated a generalizable method for the production of 3D culture tools for diverse applications including 3D culture for tissue engineering, microfluidic 3D cell culture: organs-on chips, bioreactors and 3D culture for drug screening.

Quasi-3D and 3D culture environments result in astrocyte network formation and cobblestone morphology.

The effect of 3D extracellular morphology on astrocyte morphology is well known.[9-11] However, these previous studies induce cytoskeletal change by culturing astrocytes on top of a 3D scaffold. Here, cultured astrocytes were either seeded on top of a Fmoc-DLam hydrogel or seeded on tissue culture plastic (TCP) and then covered with Fmoc-DLam hydrogel. The assembly mechanism allowing the programmed ON and OFF binary nature of our PAIN 3D culture system and its 3D morphology are shown in **Figure S1**. When astrocytes were grown underneath Fmoc-DLam, they adhered to the TCP and grew in the x and y plane but did not grow upwards into the Fmoc-DLam scaffold (referred to as quasi-3D herein). Meanwhile, astrocytes seeded on top of Fmoc-DLam also had physical interactions with Fmoc-DLam and cell media, but importantly, infiltrated the hydrogel to form a networked cobblestone morphology in the z-direction. Even though the vertical cues provided by Fmoc-DLam were available to the astrocytes in both methods of culture, it appears that only when cultured on top is a 'true-3D' environment formed. We believe, this type of cytoskeletal

organisation has never been previously reported; as such, we will refer to it as 'network formation' by astrocytes.

This network formation was observed at 24 *div,* where astrocytes grown either under or on top of Fmoc-DLam, formed networked cobblestone morphologies that were absent when cultured on two-dimensional TCP controls (**Figure 1**). Thus, the propensity of astrocytes to form networks appears to be due the presence of Fmoc-DLam, although the concentration of hydrogel in the cell media was not important (**Figure S2**). Further, we found that astrocytes could be plated at a much greater cell density (400,000 cells/well) on top of Fmoc-DLam than onto TCP under Fmoc-DLam (20,000 cells/well). The cell density of networks platted on top of Fmoc-DLam were also greater than those grown underneath Fmoc-DLam (**Figure 2B**). Astrocytes cultured on top of Fmoc-DLam grew in three-dimensions, with a corresponding increase in cell-cell and cell-material interactions, whereas those astrocytes grown underneath Fmoc-DLam were restricted to growing in the x and y plane on the TCP. We suspect that the greater cell-cell and cell- surface interactions accessed by cells plated on top of Fmoc-DLam mean that a greater plating density was accommodated and resulted in a denser astrocyte network formation. These observations suggest that the inherent properties of 3D Fmoc-DLam hydrogel (e.g. physical and biochemical features) provided the astrocytes with a microenvironment more reminiscent of the native ECM, than the 2D TCP or the 'quasi-3D' system.

The cell body areas of astrocytes grown in the 'pseudo-3D' environment was significantly greater than those grown in the 'true-3D' environment (**Figure 1C**), despite both demonstrating the networked, cobblestone morphologies as seen *in vivo*. This could be due to astrocytes flattening as they spread out on the TCP, thereby covering a greater area per cytoplasmic volume than those growing in a 3D environment, which are free to grow in the z-direction. The astrocyte network lengths were similar in each environment (**Figure 1D**) and different to the control. This demonstrates

that this cytoskeletal reorganisation was not dependent on a 3D environment, but rather an attribute of the cell-SAP interaction that was influential even in a 'pseudo-3D' environment. Our observation of astrocytes forming networks within a 3D culture environment is the first of its kind and demonstrates the potential of this biomaterial to influence immunological outcomes.

Three–dimensional cell culture environment facilitates 'in-vivo like' astrocyte network formation over time.

To probe the propensity our 3D culture system to influence astrocyte phenotype over longer term culture, 14 and 24 *div,* we also examined and compared the results to that of the quasi 3D culture system and with the morphology of astrocytes *in vivo*. After 14 *div*, astrocytes cultured on the 2D control formed flat polyclonal bodies, whilst those cultured on the Fmoc-DLam organized into clusters which formed short networks of cells - dense areas of cell nuclei ('nodes') with cellular processes extending to the next node. These networks were also observed at 24 *div*, with greater interconnectivity between each node (**Figure 2A**). As in the previous section, the three-dimensional growth of cells on Fmoc-DLam and the 2D control cultures required different seeding densities (20,000 cells/well in the 2D controls and 400,000 cells/well on Fmoc-DLam). The network cell density, calculated as (number of cells) / (area covered by F-actin^{+} staining) (**Figure 2B**), was similar regardless of the time point or the culture environment. As networks did not form in 2D, cells that were adjacent and touching each other were used to calculate cell area coverage and density. In both culture conditions, this cell density was greater than the theoretical maximum calculated from using initial seeding numbers and the total well plate area available for growth. This indicated that both systems support further growth of astrocytes at 2 and 3 weeks *in vitro*, and that Fmoc-DLam

supports a significantly greater density of growth through the provision of a third dimension. This greater density in the Fmoc-DLam cultures was accompanied by smaller cell area coverage in the x and y plane, as indicated by cell body coverage measurements (**Figure 2C**). At both time points, astrocyte cell bodies covered a significantly greater area in the 2D control compared to those grown in Fmoc-DLam, (similarly to **Figure 1C**, where astrocytes were grown underneath Fmoc-DLam), due to the flattened morphology observed on the 2D surface of TCP, compared to the more networked morphologies observed in three-dimensional Fmoc-DLam cultures. Despite this increased cell body area coverage, significantly greater networking of cells as indicated by the network length (**Figure 1D**) was observed in the Fmoc-DLam cultures. These data demonstrate the ability of Fmoc-DLam to support and maintain astrocyte cell growth for longer culture periods, with the first observation of a material induced 3D cellular network formation.

Whilst these *in vitro* results are interesting of themselves, it is important to compare these to *in vivo* astrocyte morphologies with the morphology of astrocytes in the putamen of mice 22 days after the implantation of Fmoc-DLam + 5 mg/mL fucoidan (implantation itself constituting a traumatic injury to the caudate putamen). As expected within an active injury site, astrocytes infiltrated the implanted hydrogel (**Figure 3A-B**), remarkably, replicating the networked cobblestone morphology observed *in vitro* at the same time point (**Figure 3C**). This result demonstrates the success of our novel Fmoc-DLam scaffold as a culture environment that accurately reflects the *in vivo* environment, whist also providing a platform technology to rapidly switch the behavior of *in vivo* astrocytes within an active scar to cytotrophic phenotypes. This is significant for brain repair, as we have demonstrated an ability, post injury, to rapidly convert inflammatory astrocytes back to their physiological role (i.e. supporting neurons), and in effect minimizing the detrimental functional effects of glia scar formation.

Furthermore, a desirable characteristic of an implantable material is its ability to degrade and be reabsorbed over time. Through analysis *in vitro* (**Figure 3D**), we observed an initial reduction in stiffness of the system upon seeding of cells in media and incubation at 37°C, as shown in **Figure 3D**. However, with extended incubation the elastic modulus then remained stable until 60 days, indicating that the local environment remained constant. We suggest that this initial reduction in stiffness was due to the swelling associated with the addition of cell culture media that the cells are suspended in. This is an important observation for the utility of these systems, as the modulus of the tissue should be matched after the cell suspension is added incorporated, and equilibrated.

Using Nanostructured Scaffolds to Probe and Understand the Brain Inflammatory Cascade

Having established that Fmoc-DLam hydrogel allowed astrocytes to behave in an '*in-vivo* like' fashion *in vitro*, we then demonstrated its successful utility to gain novel insights relating to astrocyte behaviour that would otherwise be impossible to obtain *in vivo*. The proliferation and metabolic activity of primary astrocytes cultured in 2D and stimulated by LPS and IL-1α was measured via an MTT metabolic assay as a proxy of the reactive behaviour of astrocytes surrounding a lesion after traumatic injury. The effects of Fmoc-DLam and its anti-inflammatory analogue Fmoc-DLamFuc (i.e. with and without fucoidan) was assessed by comparing three different groups of cultured astrocytes: i) Fmoc-DLam ii) soluble fucoidan and iii) Fmoc-DLamFuc. As expected, proliferation of astrocytes on 2D polystyrene controls were supressed when cultured with soluble fucoidan added to the media (**Figure 4A and B**) but a significant reduction was observed when Fmoc-DLamFuc was added to the culture. This was most apparent when astrocytes were stimulated by LPS ($p < 0.0001$). This is a significant result; reactive astrocytes readily proliferate, increase their expression of glial fibrillary

acidic protein (GFAP), and are hypertrophied. Therefore, the observed reduction of MTT when soluble fucoidan was presented in a reactive 2D culture and, more importantly, the significant reduction in Fmoc-DLamFuc culture indicates reduced proliferation. This supports our data (shown in **Figure 1 and 2**) where the cells expressed less GFAP and were atrophied. It also demonstrates the programmable and binary nature of our nanoscaffold in switching the inflammatory cascade as a user defined, independent variable. These results are only possible because the fucoidan is immobilised within our co-assembled system and presented to the cells via the fibrils within the Fmoc-DLam hydrogel, improving its presentation and sustaining its action. Whereas, we have previously shown that soluble fucoidan exists as a disordered polyelectrolyte 'mesh'.[33]

As well, the biologically active scaffold, Fmoc-DLam, may itself influence astrocyte metabolic activity through enabling changes in astrocyte morphology. Immunocytochemistry showed that LPS- or IL-1α-stimulated astrocytes treated with Fmoc-DLamFuc had developed a more complex network organisation than the control group (**Figure 4C**). As far as we can establish, all previous reports in the literature of astrocytes grown on TCP result in the formation of flat cells, [11] with this study being the first report of such *in vitro* cytoskeletal reorganisation. Importantly, this network formation was not observed when astrocytes were treated with soluble fucoidan (data not shown) but was also observed for the Fmoc-DLam (**Figure 4** and more strongly in **Figure 1A**) as with the Fmoc-DLamFuc (**Figure 1**), albeit with more GFAP expression and less AQP4 indicative of the culture on Fmoc-DLam having a "more reactive" phenotype. Therefore, the networked cobblestone morphology can be attributed to the presence of the Fmoc-DLam scaffold itself. As astrocyte morphology and behaviour (particularly after injury) are intimately linked, network formation and proliferation represent different phenotypic expressions of the same process that is mediated by reorganisation of the cytoskeleton and intermediate filament. In other words, in the presence of Fmoc-DLamFuc the

astrocyte proliferation is reduced with propensity for networked cobblestone "in vivo-like" morphologies being increased (**Figure 4**). This has proven the efficacy of our Fmoc-DLam 3D culture system as an accurate *in vitro* model of brain tissue, whereby we have successfully utilized it as a predictive tool to understand astrocyte behavior within an active scar site that is validated by our *in vivo* data (**Figure 3C**). This is the first report of the formation of extensive astrocyte networks *in vitro*, and the utility of a 3D culture system to study active and protracted brain inflammation.

In summary, astrocytes are known to behave differently when growing *in vivo* or on 2D cultures. Therefore, there is a critical need for 3D *in vitro* culture environments that better reflect the *in vivo* milieu, so that the physiology of astrocytes can be more readily studied, and therapeutics can be modelled. Here, we have presented a co-assembled system of Fmoc-DLam and fucoidan which has a greater suppression of LPS-stimulated astrocyte proliferation compared to soluble fucoidan, whilst also initiating morphological changes. The co-assembled system of Fmoc-DLam and fucoidan suppresses astrocyte proliferation induced by LPS and leads to extensive networks of fibres formed by the astrocytes. The network formation depends on the presence of Fmoc-DLam and is observable *in vivo* within an active scar site. Fmoc-DLam represents a biomimetic programmable 3D culture environment and tissue engineering construct of particular significance to immunological and regenerative medicine research.

Experimental Section

Gel formation

5mg Fmoc-DIKVAV (99% desalted, Pepmic, China) and 2 or 5 mg/mL fucoidan (Marinova, Australia) was dissolved in 400 L deionized water, to which 30 L 0.5M sodium hydroxide (Bacto, Australia) was

added. 95 L 0.1M hydrochloric acid (Merck, Australia) was then added dropwise to slowly reduce the pH with continuous vortexing. Once physiological pH was reached (measured with a microprobe pH meter), hydrogels were exposed to UV for two hours, after which the final volume was reached using Dulbecco's Modified Eagle's Medium High Glucose (DMEM, HyClone, United Kingdom) ready for immediate use in culture.

Primary astrocyte cell culture

Primary astrocyte cell culture was conducted as previously described [34]. Briefly, postnatal day 1.5-2 Swiss mice pups were sacrificed, and their forebrains were dissected in cold DMEM High Glucose (HyClone). Tissue was dissociated and centrifuged for 10 minutes at 1000 rpm and resuspended in CDMEM 10:10:1 (completed DMEM, 10% fetal bovine serum (Gibco), 10% horse serum (Gibco), 1% penicillin/streptomycin (Hyclone) at 37°C, with 15 mL per forebrain. Cells were plated on poly-d-lysine (PDL) coated T75 flasks, with 15 mL cell suspension per flask. Cells were maintained at 37°C and 5% CO_2 for two weeks.

At 14 *div,* with a confluent cell layer, media was changed and left to equilibrate in the incubator for 2-3 hours, after which the flask lid was sealed with parafilm and the flask was placed on an orbital shaker (230 rpm at 37°C) overnight. Media was then removed, washed once with PBS (1X) to remove non-astrocytic cells. Astrocytes were detached from the flask using 3 mL trypsin (4 minutes at 37°C, HyClone), added to 15 mL CDMEM 5:5:1 (5% fetal bovine serum (Gibco), 5% horse serum (Gibco), 1% penicillin/streptomycin (Hyclone) and centrifuged for 10 minutes at 1000 rpm. The resultant cell pellet was resuspended in 3 mL CDMEM 5:5:1 and cell counts were performed with 10 µL cell suspension, 10 µL PBS, and 80 µL trypan blue. Cells were seeded as per details in the following

sections. For details on LPS and IL-1a stimulation and MTT assay experimental details please refer to supplementary information.

Gel exposure experiments

To investigate the effect of Fmoc-DIKVAV on cell morphology and organization when on top of astrocytes, cells were seeded at 10,000 cells/well in 48 well plates and maintained for 2-3 weeks prior to hydrogel exposure to ensure there was a confluent layer to observe changes. Hydrogels were prepared as described above, and diluted at 10, 20, 40, 60, and 80% in CDMEM 5:5:1. Media was removed from cells, with 150-200 µL hydrogel dilutions added to each well.

Cells were maintained for 7 days with the gel ("Gel on"), then removed for 7 days and replaced with media ("Gel on-off"), and then replaced again with hydrogel ("Gel on-off-on"). For the "Gel on" group, hydrogel solutions were replenished every 7 days.

Three-dimensional cultures

To grow astrocytes in a three-dimensional (3D), Fmoc-DIKVAV hydrogels were plated on top of PDL-coated TCP. 200-400 L of hydrogel was added to each well and left under UV in a Biosafety Cabinet II for 2 hours, with the well plate lids off, and then incubated overnight to equilibrate. Cells were then seeded on top of the hydrogels the next day (400,000 cells/well for a 24 well plate) and maintained for 14 or 24 days. 2D controls were seeded at 20,000 cells/well (in 24 well plates). Please refer to supplementary information for details of the immunohistochemistry procedure and network analysis.

Statistical analysis

All values presented are mean ± SEM. Data were subjected to 2-way ANOVA or unpaired t-tests using Prism v6.0 (GraphPad, USA).

Stab injury and hydrogel implantation

C57 BL/6 mice (male and female) were anaesthetised with 1-2% Isoflurane. Once in a stereotaxic frame, a small hold was drilled into the skull, followed by the lowering of a 21G needle attached to a Hamilton needle into the RHS striatum (co-ordinates AP+0.5 mm, L-2.0 mm, deep -3.0 mm from bregma) to create the stab injury. Hydrogels were exposed to UV for 20 minutes prior to implantation, and were drawn up into a Hamilton syringe, which was attached to a fine glass capillary. 3 µL of hydrogel was injected into the stab injury, in increments of 0.5 µL/0.5 mm, moving upwards.

Tissue preparation

Mice were perfused 21 days post-implantation with warmed (37 °C) 0.1 M PBS, followed by 35 mL of chilled 4% PFA (Sigma Aldrich) in 0.1 M PBS and 0.2% picric acid (4°C; pH 7.4). Brains were post-fixed for one hour, left for two nights at 4°C in a 30% sucrose PBS solution. Frozen brains were cryosectioned at 20 µm thick in a 1:10 series on to slides double coated with 0.1% chrome alum

(Ajax Chemicals) and 1% gelatine (Sigma Aldrich). Please refer to supplementary information for details of the immunohistochemistry procedure for the primary tissue.

Gel incubation

400 μL/well of Fmoc-DIKVAV hydrogel was transferred into 48-well plates and 200 μL of PBS was added on top of the hydrogel. Hydrogels were incubated at 37°C and 5% CO_2 incubation for 21 or 60 days and PBS was replenished every 3-4 days.

Rheological testing

The viscoelastic properties of the control and incubated hydrogels were determined used a Kinexus Pro+ Rheometer (Malvern), with a 20 mm smooth flat plate with a solvent trap. The PBS supernatant was removed from each well, after which the Fmoc-DIKVAV gel was placed on the plate and left at room temperature for 2 minutes. A 0.2 mm loading gap was used with a shear strain of 0.4% and a frequency of 0.1 – 100 Hz.

Supporting Information

Supporting Information is available from the Wiley Online Library or from the author.

Acknowledgements

This research was supported by funding from an NHMRC project grant (GNT1144996) and an ARC discovery project (DP130103131). FLM was supported by an Australian Postgraduate Award; MKH was supported by a NHMRC Research Fellowship GNT1020401; DRN was supported by a NHMRC Dementia Research Leadership Fellowship (GNT1135687). Access to the facilities of the Australian National University Centre for Advanced Microscopy (CAM) with funding through the Australian Microscopy and Microanalysis Research Facility (AMMRF) is gratefully acknowledged. Finally, we greatly acknowledge Marinova Pty Ltd, Cambridge, Tasmania, Australia for the supply of fucoidan.

References

[1] E. A. Gosselin, H. B. Eppler, J. S. Bromberg, C. M. Jewell, Nat. Mater. 2018, 17, 484.

[2] H. Tekin, S. Simmons, B. Cummings, L. Gao, X. Adiconis, C. C. Hession, A. Ghoshal, D. Dionne, S. R. Choudhury, V. Yesilyurt, N. E. Sanjana, X. Shi, C. Lu, M. Heidenreich, J. Q. Pan, J. Z. Levin, F. Zhang, Nat. Biomed. Eng. 2018, 2, 540; M. Su, Z. Huang, Y. Li, X. Qian, Z. Li, X. Hu, Q. Pan, F. Li, L. Li, Y. Song, Adv. Mater. 2018, 30, 1703963; X Hu, Z. Huang, X. Zhou, P. Li, Y. Wang, Z. Huang, M. Su, W. Ren, F. Li, M. Li, Y. Chen, Y. Song, Adv. Mater., 2017, 29, 1703236; Z. Huang, M. Su, Q. Yang, Z. Li, S. Chen, Y. Li, X. Zhou, F. Li, Y. Song, Nat. Commun. 2017, 8, 14110.

[3] C. M. Madl, S. C. Heilshorn, H. M. Blau, Nature 2018, 557, 335; L. Gong, L. Cao, Z. Shen, L. Shao, S. Gao, C. Zhang, J. Lu, W. Li, Adv. Mater. 2018, 30, 1705684; Z. Liu, M. Tang, J. Zhao, R. Chai, J. Kang, Adv. Mater. 2018, 30, 1705388.

[4] A. Almad, N. J. Maragakis, Nat Rev Neurol 2018, 14, 351.

[5] L. R. Nih, E. Sideris, S. T. Carmichael, T. Segura, Adv. Mater. 2017, 29.

[6] J. E. Burda, M. V. Sofroniew, Neuron 2014, 81, 229; M. V. Sofroniew, H. V. Vinters, Acta Neuropathol. (Berl.) 2010, 119, 7; J. R. Faulkner, J. E. Herrmann, M. J. Woo, K. E. Tansey, N. B. Doan, M. V. Sofroniew, J Neurosci 2004, 24, 2143; S. Okada, M. Nakamura, H. Katoh, T. Miyao, T. Shimazaki, K. Ishii, J. Yamane, A. Yoshimura, Y. Iwamoto, Y. Toyama, Nat. Med. 2006, 12, 829.

[7] J. W. Salatino, K. A. Ludwig, T. D. Y. Kozai, E. K. Purcell, Nat. Biomed. Eng. 2017, 1, 862.

[8] P. Q. Nguyen, N. M. D. Courchesne, A. Duraj-Thatte, P. Praveschotinunt, N. S. Joshi, Adv. Mater. 2018, 30.

[9] C. L. Lau, M. Kovacevic, T. S. Tingleff, J. S. Forsythe, H. S. Cate, D. Merlo, C. Cederfur, F. L. Maclean, C. L. Parish, M. K. Horne, D. R. Nisbet, P. M. Beart, J. Neurochem. 2014, 130, 215.

[10] R. D. O'Shea, C. L. Lau, N. B. Zulaziz, F. L. Maclean, D. R. Nisbet, M. K. M. Horne, P. M. Beart, Front. Neurosci. 2015, 9, 50.

[11] T. B. Puschmann, C. Zandén, Y. De Pablo, F. Kirchhoff, M. Pekna, J. Liu, M. Pekny, Glia 2013, 61, 432.

[12] J. M. Zuidema, M. C. Hyzinski-García, K. Van Vlasselaer, N. W. Zaccor, G. E. Plopper, A. A. Mongin, R. J. Gilbert, Biomaterials 2014, 35, 1439.

[13] F. Maclean, R. Williams, M. Horne, D. Nisbet, Neurochem. Res. 2015, 41, 589.

[14] D. R. Nisbet, R. J. Williams, Biointerphases 2012, 7, 1.

[15] A. P. Balgude, X. Yu, A. Szymanski, R. V. Bellamkonda, Biomaterials 2001, 22, 1077; K. J. Lampe, R. G. Mooney, K. B. Bjugstad, M. J. Mahoney, J. Biomed. Matter. Res. A 2010, 94A, 1162; M. C. LaPlaca, D. K. Cullen, J. J. McLoughlin, R. S. Cargill Ii, J. Biomech. 2005, 38, 1093; M. J. Mahoney, K. S. Anseth, J. Biomed. Matter. Res. A 2007, 81A, 269; D. R. Nisbet, K. E. Crompton, M. K. Horne, D. I. Finkelstein, J. S. Forsythe, J Biomed Mater Res B Appl Biomater. 2008, 87, 251.

[16] A. Hsieh, T. Zahir, Y. Lapitsky, B. Amsden, W. Wan, M. S. Shoichet, Soft Matter 2010, 6, 2227; T.-Y. Wang, K. F. Bruggeman, J. A. Kauhausen, A. L. Rodriguez, D. R. Nisbet, C. L. Parish, Biomaterials 2016, 74, 89.

[17] A. Tuladhar, M. S. Shoichet, Nat. Mater. 2018, 17, 573.

[18] R. J. Wade, E. J. Bassin, W. M. Gramlich, J. A. Burdick, Adv. Mater. 2015, 27, 1356.

[19] S. Koutsopoulos, S. Zhang, Acta Biomater. 2013, 9, 5162; A. L. Rodriguez, C. L. Parish, D. R. Nisbet, R. J. Williams, Soft Matter 2013, 9, 3915.

[20] R. Li, S. Pavuluri, K. Bruggeman, B. M. Long, A. J. Parnell, A. Martel, S. R. Parnell, F. M. Pfeffer, A. J. C. Dennison, K. R. Nicholas, C. J. Barrow, D. R. Nisbet, R. J. Williams, Nanomed. Nanotechnol. Biol. Med. 2016, 12, 1397.

[21] V. Modepalli, A. Rodriguez, R. Li, S. Pavuluri, C. Barrow, D. Nisbet, R. Williams, Pept. Sci. 2014, 101, 197.

[22] X. Q. Dou, C. L. Feng, Adv. Mater. 2017, 29.

[23] Y. Jin, J. S. Lee, J. Kim, S. Min, S. Wi, J. H. Yu, G.-E. Chang, A.-N. Cho, Y. Choi, D.-H. Ahn, S.-R. Cho, E. Cheong, Y.-G. Kim, H.-P. Kim, Y. Kim, D. S. Kim, H. W. Kim, Z. Quan, H.-C. Kang, S.-W. Cho, Nat. Biomed. Eng. 2018, 2, 522.

[24] J. Boekhoven, S. I. Stupp, Adv. Mater. 2014, 26, 1642; S. Koutsopoulos, J. Biomed. Matter. Res. A 2016, 104, 1002; R. J. Mart, R. D. Osborne, M. M. Stevens, R. V. Ulijn, Soft Matter 2006, 2, 822.

[25] G. Wei, Z. Q. Su, N. P. Reynolds, P. Arosio, I. W. Hamley, E. Gazit, R. Mezzenga, Chem. Soc. Rev. 2017, 46, 4661.

[26] C. C. Horgan, A. L. Rodriguez, R. Li, K. F. Bruggeman, N. Stupka, J. K. Raynes, L. Day, J. W. White, R. J. Williams, D. R. Nisbet, Acta Biomater. 2016, 38, 11.

[27] K. F. Bruggeman, A. L. Rodriguez, C. L. Parish, R. J. Williams, D. R. Nisbet, Nanotechnology 2016, 27, 385102.

[28] R. Li, N. L. McRae, D. R. McCulloch, M. Boyd-Moss, C. J. Barrow, D. R. Nisbet, N. Stupka, R. J. Williams, Biomacromolecules 2018, 19, 825.

[29] A. L. Rodriguez, T.-Y. Wang, K. F. Bruggeman, R. Li, R. J. Williams, C. L. Parish, D. R. Nisbet, Nano Research 2016, 9, 674.

[30] F. A. Somaa, T. Y. Wang, J. C. Niclis, K. F. Bruggeman, J. A. Kauhausen, H. Guo, S. McDougall, R. J. Williams, D. R. Nisbet, L. H. Thompson, C. L. Parish, Cell Rep. 2017, 20, 1964.

[31] H. Y. Park, M. H. Han, C. Park, C.-Y. Jin, G.-Y. Kim, I.-W. Choi, N. D. Kim, T.-J. Nam, T. K. Kwon, Y. H. Choi, Food Chem. Toxicol. 2011, 49, 1745.

[32] F. L. Maclean, Y. Wang, R. Walker, M. K. Horne, R. J. Williams, D. R. Nisbet, ACS Biomater Sci Eng. 2017, 3, 2542.

[33] R. Li, M. Boyd-Moss, B. Long, A. Martel, A. Parnell, A. J. C. Dennison, C. J. Barrow, D. R. Nisbet, R. J. Williams, Sci Rep 2017, 7, 4797.

[34] M. Mecha, P. M. Iñigo, L. Mestre, M. Hernangómez, J. Borrell, C. Guaza, 2011.

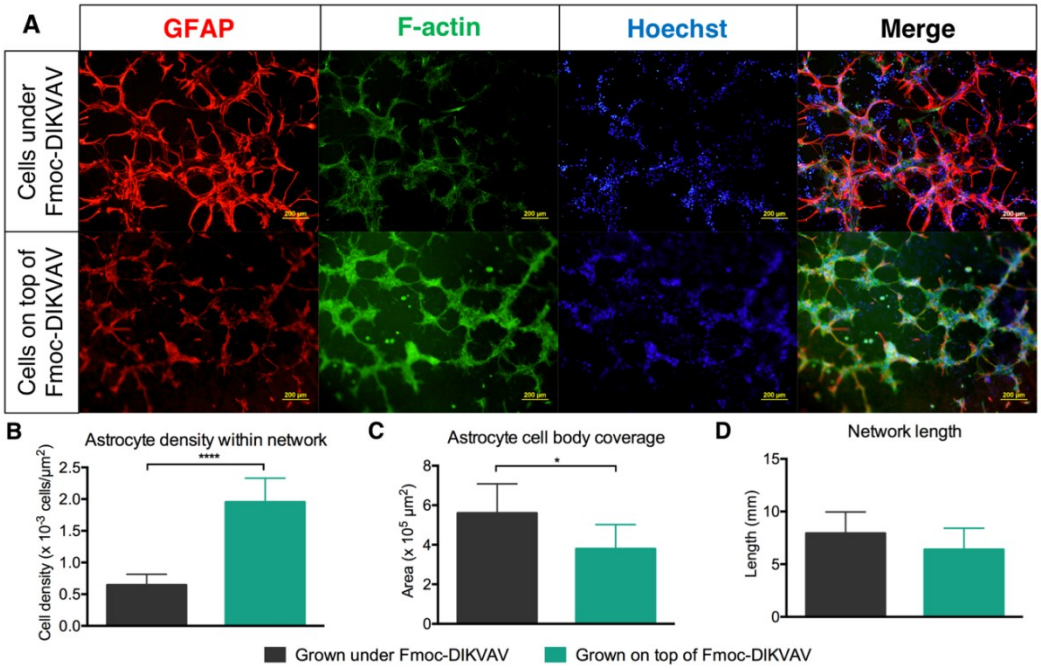

Figure 1. Astrocyte networks form when grown underneath or on top of Fmoc-DLam for 24 *div*, but not in a 2D environment. When astrocytes were grown underneath Fmoc-DLam (Figure S1 A -top row), they initially adhered to the TCP prior to the hydrogel being cast over the top. As a result, they grew in the x and y plane but did not grow upwards into the Fmoc-DLam scaffold (referred to as quasi-3D). Importantly, cytoskeletal reorganisation from a reactive to a cytotrophic phenotype, reminiscent of astrocyte in the uninjured brain, resulted after Fmoc-DLam was cast over the reactive 2D culture. Meanwhile, astrocytes seeded on top of Fmoc-DLam in a 3D culture (Figure S1 A - second row) had initial physical interactions with Fmoc-DLam and cell media, and as such infiltrated the hydrogel to form a networked cobblestone (cytotrophic) morphology in the z-direction. Our observation of astrocytes forming networks within a 3D culture environment is the first of its kind. A) Immunocytochemistry of GFAP (red), F-actin (green), Hoechst (blue), and merge. B) Astrocyte density within the cell networks. C) Area covered by astrocyte cell bodies within the network. D) Network length of astrocytes. Scale bar = 200 µm, values are mean ± SEM.

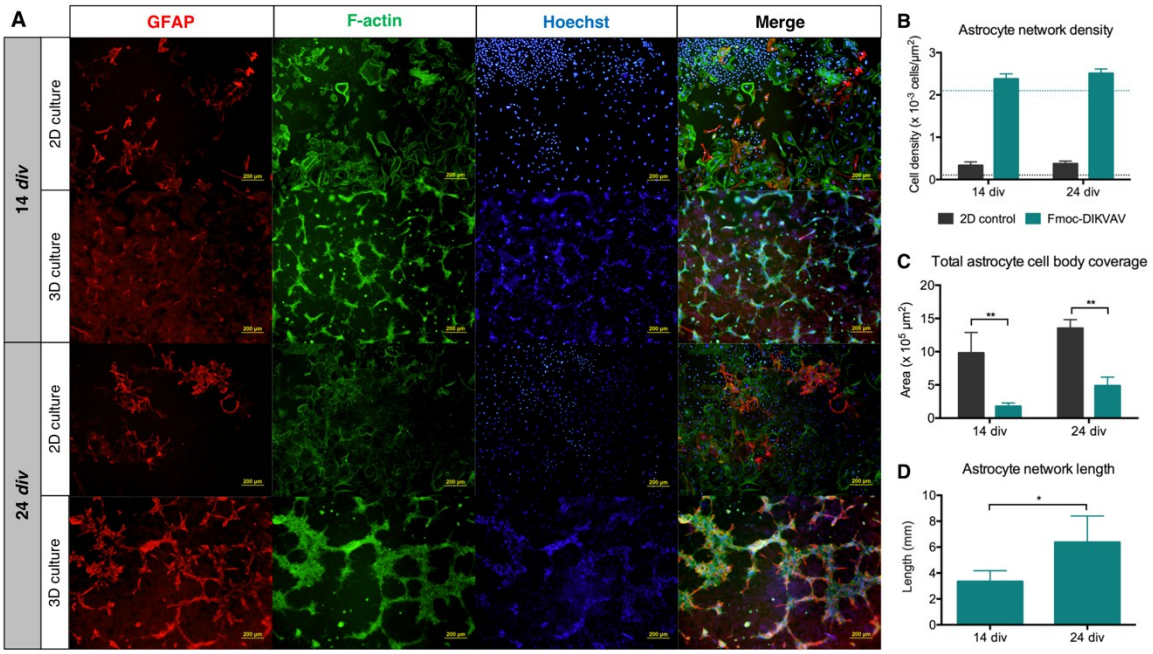

Figure 2. Primary astrocytes cultured for 14 or 24 div on 2D TCP or 3D Fmoc-DLam hydrogel. A) Immunocytochemistry of: GFAP (red), F-actin (green), Hoechst (blue), and merge. B) Astrocyte density, dotted lines indicated theoretical maximum initial seeding density. C) Total area covered by astrocytes cell bodies. D) Network length of astrocytes grown on Fmoc-DLam. Scale bar = 200 µm, values are mean ± SEM.

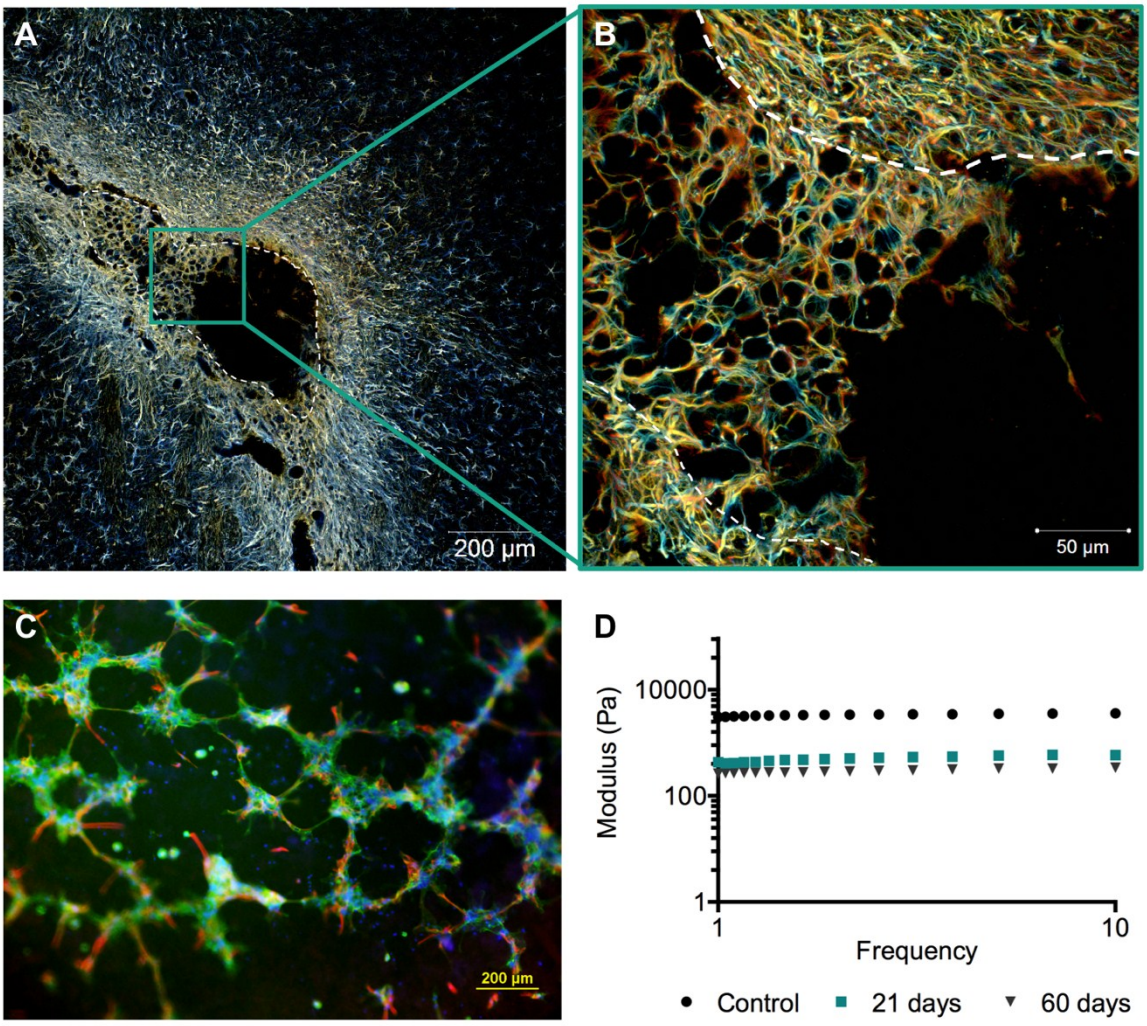

Figure 3. Astrocyte network formation at A) 22d post injury and implantation of Fmoc-DLam + 5 mg/mL fucoidan, B) Zoomed field of view of the network (depth colour coded projection of GFAP+ astrocytes), C) 24 *div* cultured on top of Fmoc-DLam, immunostaining of GFAP (red), F-actin (green), and Hoechst (blue), and D) Storage moduli of Fmoc-DLam control (no incubation) or Fmoc-DLam incubated for 21 and 60 days.

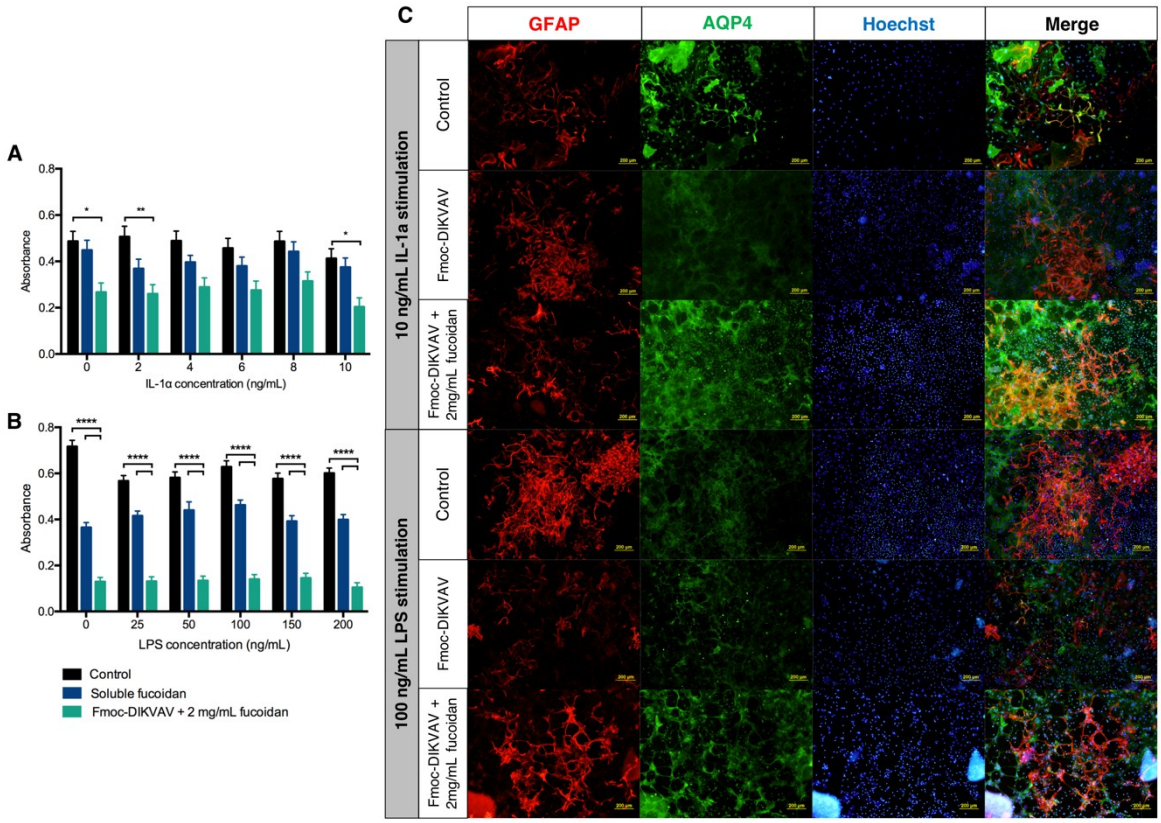

Figure 4. Fmoc-DLam co-assembled with 2 mg/mL fucoidan exhibits exerts anti-proliferative and cell-reorganisation effects on astrocytes *in vitro*. Metabolic activity of A) 10 ng/mL IL-1α-stimulated and B) 100 ng/mL LPS-stimulated astrocytes treated with nothing (control), soluble fucoidan, or Fmoc-DLam + 2mg/mL fucoidan. C) Immunocytochemistry of: GFAP (red), Aquaporin-4 (AQP4) (green), Hoechst (blue), and merge. Values are mean ± SEM, scale bar = 200 µm, * $p < 0.05$, ** $p < 0.01$, **** $p < 0.0001$.

A programmed anti-inflammatory nanoscaffold with valuable properties that allow tissue independent switching of the inflammatory cascade is presented. This is demonstrated within an active scar site, due to the resilience of the nanoscaffold to the presence of inflammatory cells and enzymes. Efficacy is established via previously unattainable insights about inflammatory cells, which is impossible to obtain via *in vivo* experimentation.

Keyword: 3D cell culture, nanoscaffolds, regenerative medicine, disease modeling, inflammation

Dr F. L. Maclean[1], Ms G. M. Ims[1], Professor M. K. Horne[2,3], Dr R. J. Williams[4,5], and Associate Professor David R. Nisbet[1,2,5]

[1]Laboratory of Advanced Biomaterials, Research School of Engineering, The Australian National University, Canberra, Australia, 2601. [2]Florey Institute of Neuroscience and Mental Health, University of Melbourne, Parkville, Australia, 3052. [3]Department of Medicine, University of Melbourne, St Vincent's Hospital, Fitzroy, Australia, 3065. [4]School of Engineering, RMIT University, Melbourne, Australia, 3000. [5]BioFab3D, St Vincent's Hospital, Fitzroy, Australia, 3065.

Dr R.J. Williams and Associate Professor D. R. Nisbet had equal contribution.

Corresponding Author: E-mail: david.nisbet@anu.edu.au, Associate Professor D. R. Nisbet[1,2,5], richard.williams@rmit.edu.au, Dr R. J. Williams[4,5]

Programmed anti-inflammatory nanoscaffold (PAIN) as a 3D tool to understand the brain injury response.